3.33 Modeling of Olfactory Processing ☆

Christiane Linster[a] and Thomas A Cleland[b], [a] Department of Neurobiology and Behavior, Cornell University, Ithaca, NY, United States; and [b] Department of Psychology, Cornell University, Ithaca, NY, United States

Glossary

Associative memory In this context, the term refers to a type of neural network in which associations between different elements of a stimulus are stored by strengthening connections between these elements. The most important feature of an associative memory is that it will restore a previously stored pattern when presented with an incomplete or distorted version of this pattern.

Attractor In dynamical systems analysis, an attractor is any state of a system in which it will remain if otherwise undisturbed. The attractor of a simple pendulum is the vertical position; adding magnets or other disturbances to the system may move the attractor to a new position, or generate additional attractors. Attractors need not be single points; cyclic attractors are common.

Hebbian learning A type of plasticity ("learning") rule in which interactions between simultaneously active elements, such as neurons, are strengthened incrementally.

Molecular receptive range Equivalent to receptive field for different chemical ligands. In the olfactory system, a neuron's molecular receptive range describes the ensemble of chemicals to which it is responsive.

Olfactory bulb Cortical telencephalic structure receiving direct afferent input from olfactory sensory neurons located in the nasal cavity, as well as efferent input from multiple regions of the brain.

Signal-to-noize ratio Engineering term quantifying the proportion of the signal of interest (signal) in the total information stream that is transmitted (signal + noise). Low signal-to-noize ratios render it difficult to detect or interpret the signal, as it is buried in noise.

3.33.1 Abstract

Computational models are increasingly essential to systems neuroscience. Models serve as proofs of concept, tests of sufficiency, and as quantitative embodiments of working hypotheses, and are important tools for understanding and interpreting complex datasets. In the olfactory system, models have played a particularly prominent role in framing contemporary theories and presenting novel hypotheses. As the complexity and intricacy of experimental data continue to increase, the importance of computational modeling will continue to grow. We here review computational models of olfactory processing with a view to the computational role, functionality and brain area studied. We discuss what types of insights can be gained from different levels of computational modeling. We specifically discuss the computations necessary to perform filtering and contrast enhancement operations, the role of synchrony and dynamics for computational purposes as well associative memory function. Large scale simplified neural networks as well as detailed biophysical models are compared and discussed.

3.33.2   Introduction

In natural environments, airborne chemical stimuli are distributed unpredictably in time and space, and odorants from innumerable sources intermix freely. The olfactory system must be able to detect potential signals of interest within these chemically noisy environments, correctly extract these signals from a complex and changing odor background to form stimulus representations, compare these constructed representations to those of previously experienced odors, differentiate relevant from irrelevant stimuli, and cue an appropriate response. Many of the neural circuit elements comprising the olfactory system contribute to these processes; in particular, multiple feedback and feedforward interactions among olfactory structures, as well as between olfactory and non-olfactory areas, are thought to contribute to the filtering and construction of olfactory representations. Computational models of olfactory processing have been increasingly utilized to describe and interpret these complex and interrelated phenomena.

Primary olfactory sensory neurons (OSNs) number in the millions in rodents. Their axons are highly convergent, targeting specific, discrete neuropilar synaptic regions within the input layer of the olfactory bulb known as glomeruli. In hamsters, for example, between 1300 and 4700 OSNs believed to express the same odorant receptor complement converge upon each glomerulus (Schoenfeld and Knott, 2004). These large populations of redundant OSNs and their correspondingly high convergence ratios have been proposed to yield advantages such as improved stimulus sensitivity, an improved signal to noise ratio, and an increased range of tuning to different odorant concentrations (Cleland and Linster, 1999; Duchamp-Viret et al., 1989; Meisami, 1989; van Drongelen et al., 1978). The molecular receptive ranges, or chemical receptive fields, of these odorant receptors overlap substantially, such that the identity of odorants is not associated with the activation of a specific receptor, but rather is represented by a distributed, combinatorial code (Adrian, 1953; Kauer, 1991; Moulton, 1967; Stewart et al., 1979), now recognized as a pattern of activation across many receptors. Owing to the specific convergence of OSN axons, these odor-specific activity patterns can be most clearly observed in imaging studies of olfactory bulb glomeruli (Fletcher and Bendahmane, 2014; Friedrich and Korsching, 1997; Meister and Bonhoeffer, 2001; Rubin and Katz, 1999; Wachowiak et al., 2002). These overlapping representations underlie two critical properties of the olfactory system that a labeled-line solution would not. First, the number of unique odor representations is not limited to the number of different receptor types (roughly 1000 in mice (Mombaerts, 1996), but can be estimated as m^n, where n denotes the number of receptor types and m denotes the number of recognizable states that each sensor can assume, ultimately limited by the signal to noise ratio of the system. Even if only two receptor states, active and inactive, are recognized, this enables roughly 2^{1000} potential odor stimuli to be represented in mice. Second, the fact that structurally and perceptually similar odorant molecules will activate correspondingly overlapping sets of olfactory establishes a basis for the recognition of stimulus similarity in the olfactory system receptors (Cleland et al., 2002; Linster et al., 2002; 2001). This is a prerequisite for basic postsensory cognitive processes such as generalization (Cleland et al., 2002, 2009; Shepard, 1987; Shepard and Chang, 1963) and a tolerance for variance among repeated stimulus samples that a labeled-line system would have no clear means of generating.

Distributed patterns of activity in response to chemical stimuli are transmitted to the olfactory bulb via OSN axons that terminate in the glomeruli of its input layer. The olfactory bulb is believed to filter and transform these incoming sensory data, performing normalization, contrast enhancement, and similar operations before conveying the processed olfactory information to several different secondary olfactory structures via mitral cell axon collaterals (Cleland and Linster, 2003; Nagayama et al., 2014). Notably, the bulb constitutes the last common stage at which olfactory sensory representations can be processed before the signal diverges dramatically into these multiple secondary structures. It is clear from recent investigations that the perceptual qualities of odorants can be predicted, to a limited degree, from the patterns of activation that they evoke at the olfactory bulb input layer (Cleland et al., 2002; Linster and Hasselmo, 1999; Linster et al., 2001, 2002). However, several aspects of odor perception, e.g., changes in perception and discrimination capacity due to odor intensity or prior experience, cannot be predicted solely by this first-order representation as reflected in glomerular activation patterns (Cleland et al., 2009). Furthermore, the olfactory bulb receives substantial centrifugal projections from both cortical and neuromodulatory centers, and its activity is strongly regulated by learning and experience. It is therefore safe to assume that the olfactory bulb plays an important role in processing incoming sensory information. Indeed, many models of olfactory bulb signal processing have been developed, which are grouped here into studies of (1) filtering and contrast enhancement, (2) mechanisms underlying oscillations and spike synchronization, and (3) odor segmentation and associative memory function. In addition, a number of detailed biophysical models of bulbar neurons have been constructed, in many cases to address how their intrinsic properties underlie and interact with network properties.

3.33.3   Filtering and Contrast Enhancement

The high convergence ratio between OSNs expressing a particular odorant receptor and their target glomeruli in the olfactory bulb (Fig. 1A) is believed to improve the signal to noise ratio during odorant detection (van Drongelen et al., 1978), potentially overcoming the limiting noise inherent in the transduction mechanisms of individual OSNs (Lowe and Gold, 1995). In principle, this property improves the coding capacity of the olfactory system, increasing the number of different odor-specific patterns that can be discriminated, as well as improving the maximum reliable sensitivity of the system (Fig. 1B). Another modeling study has suggested that this same property can be employed to increase the range of odor ligand concentrations that can be represented by olfactory bulb glomeruli without saturation (Fig. 1C) (Cleland and Linster, 1999). This hypothesis provides a possible answer to the conundrum of how collective concentration-response curves measured by glomerular imaging can be substantially broader than those measured in individual OSN recordings (Bozza et al., 2002; Friedrich and Korsching, 1997), enabling preservation of the ratios
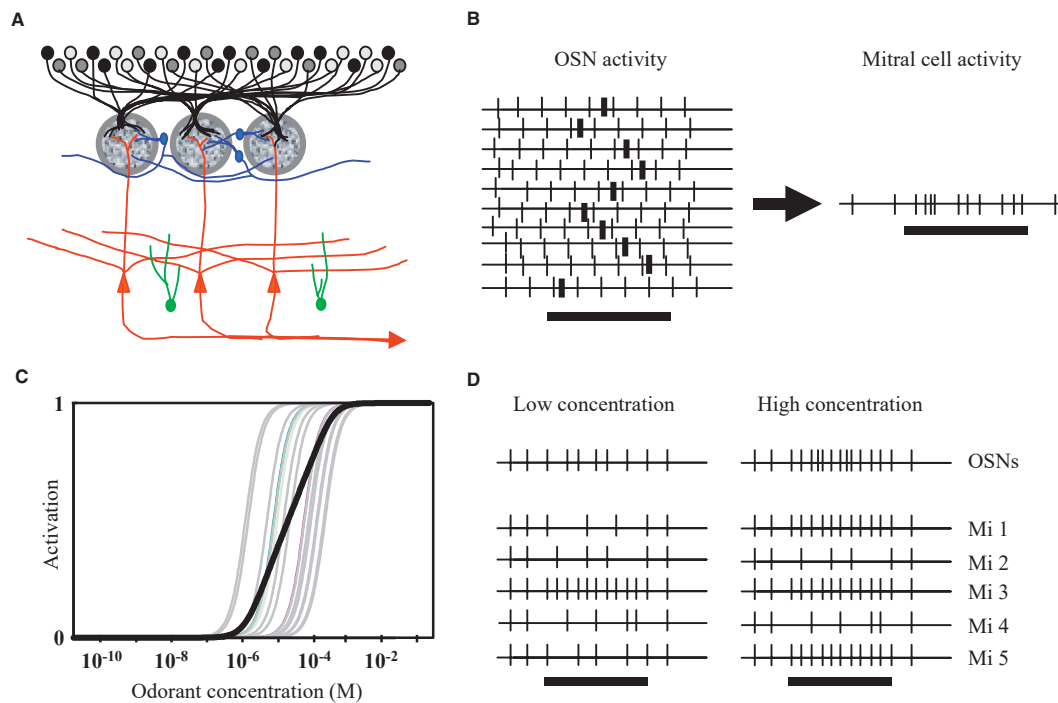
Figure 1   Glomerular computations and convergence. (A) Simplified structure of the olfactory bulb as represented in most computational models. Large populations of OSNs expressing the same receptor (particular shades of gray) converge onto common glomeruli in the olfactory bulb, within which they synapse onto the dendrites of periglomerular (blue) and mitral (red) cells. Mitral cells also excite granule cells (green) via their lateral dendrites, and granule cells in turn inhibit mitral cells; functionally, this mediates lateral inhibition between mitral cells. Periglomerular cells are primarily associated with one or a small number of glomeruli and project axons to a few other glomeruli; these have also been suggested to mediate lateral inhibition between mitral cells. A number of other cell types have also been characterized in the bulb, such as short-axon and tufted cells, that are rarely included in computational models; furthermore, established heterogeneity within the cell types modeled has usually been neglected. (B) The high convergence of OSN axons onto mitral cells within each glomerulus significantly improves the signal-to-noize ratio in mitral cells as compared to OSNs. Even if a weak odorant stimulus were to evoke only a single additional spike in each OSN above its basal rate of spiking (*OSN activity*; bold lines), this high convergence ratio can generate a robust odor responses in a postsynaptic mitral cell (*Mitral cell activity*), hence enabling mitral cells to reliably represent odor stimuli at lower concentrations than can OSNs (van Drongelen et al., 1978). Horizontal bars depict the time of odorant presentation. (C) While OSN concentration-activation curves are steep, enabling accurate representations of ligand-receptor binding over a range of roughly one log unit concentration, the considerably broader curves observed in glomeruli can be explained if the convergent OSN population is nonuniform in spare receptor capacity or other determinants of intracellular gain (Cleland and Linster, 1999). If OSNs with identical odorant selectivity but exhibiting different functional spare receptor capacities (gray sigmoids) project onto a single glomerulus, the summed concentration-activation curve of that glomerulus can span several log units of concentration (black sigmoid). (D) Frequency-to-spatial transformation by local glomerular circuits would activate different populations of mitral cells within each glomerulus as a function of the average firing rate of the convergent OSNs (Anton et al., 1991). Low concentration odorants (left panel) evoke weak activity in a given receptor-specific OSN subpopulation, generating increased activity in only one mitral cell. In contrast, a high concentration odor stimulus (right panel) evokes greater activity in the OSN population and hence generates measurable excitatory responses in three mitral cells. Horizontal bars depict the time of odorant presentation.

of activation levels among glomeruli across broader concentration ranges and hence potentially facilitating the recognition of odor quality across changes in concentration (Cleland et al., 2011; Cleland et al., 2007). Another approach has been suggested by Anton et al., (1991). Noting that the activity of each glomerulus is sampled and conveyed centrally by a number of mitral cells (on the order of 50 in hamsters (Schoenfeld and Knott, 2004)), and that mitral cell firing frequencies do not scale monotonically with concentration as do those of OSNs, these authors proposed that the synaptic circuitry within each glomerulus could compute a frequency-to-spatial transformation on the incoming information. That is, the number of responding mitral cells within a glomerulus, but not their firing rate, would depend on the firing rates of the sensory neurons projecting to that glomerulus in response to odor stimulation (Fig. 1D).

Contrast enhancement is a common property of sensory systems that narrows, or sharpens, sensory representations by specifically inhibiting neurons on the periphery of the representation, hence enhancing the contrast between signal and background. A number of computational models have investigated the contrast enhancement potential of olfactory bulb circuitry (Fig. 2A), most of which, by analogy with the retina, have investigated the potential role of lateral inhibitory projections. Classically, bulb models have emphasized lateral inhibition mediated by mitral cell lateral dendrites (Davison et al., 2003; Rall and Shepherd, 1968; Schild, 1988; Shepherd and Brayton, 1979; Urban, 2002). These lateral dendrites form reciprocal synapses with inhibitory granule cell spines in the external plexiform layer of the bulb, forming a network through which mitral cells inhibit one another
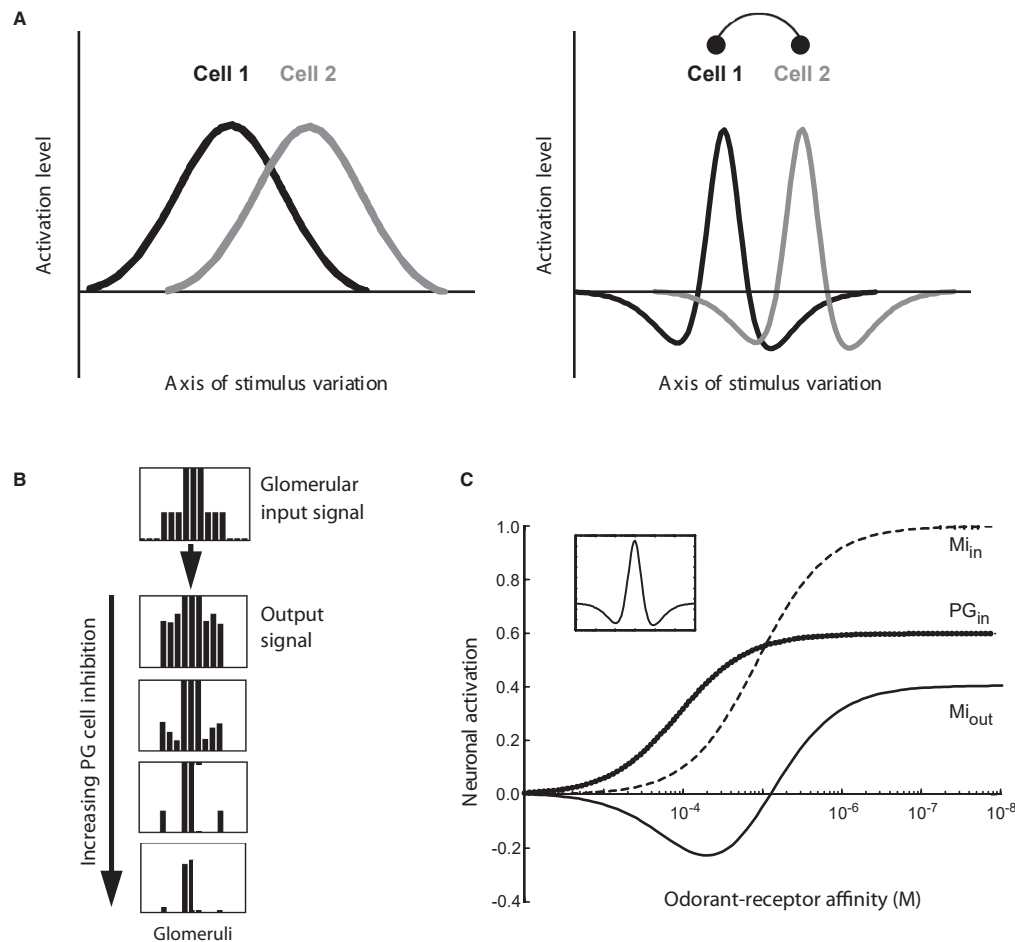
Figure 2   Contrast enhancement. (A) Contrast enhancement is a phenomenon observed in most sensory systems by which marginally activated neurons are excluded from a stimulus-specific ensemble by inhibition, hence sharpening the sensory representation and differentiating it from other, similar representations. In the absence of contrast enhancement, the tuning curves of cells 1 and 2 substantially overlap (left panel). If contrast enhancement is enabled, e.g., by the addition of lateral inhibition such that each cell inhibits the other, the two cells both become more narrowly tuned, and their receptive fields may no longer overlap (right panel). (B) Computational models of the olfactory bulb have proposed that inhibitory periglomerular (PG) cells could mediate contrast enhancement in the glomerular layer of the olfactory bulb. In these models, PG cells receive direct sensory input within a given glomerulus and inhibit mitral cells in neighboring glomeruli via axonal projections (**Fig. 1**A). If an odor stimulus activates a range of neighboring glomeruli (*Glomerular input signal*), increasing the level of PG cell-mediated inhibition would lead to concomitantly sharpened representations among mitral cells, the output layer of the olfactory bulb. With strong contrast enhancement, only the most strongly activated mitral cells are activated, while weakly activated mitral cells are inhibited (Linster and Gervais, 1996; Linster and Hasselmo, 1997). (C) Non-topographical contrast enhancement based on local glomerular computations. In this model, contrast enhancement is generated within the stimulus-response profile of each individual glomerulus, resulting in sharpening of the odor-evoked representation across the glomerular layer. Within each glomerulus, mitral (Mi_{in}) and periglomerular (PG_{in}) cells have the same tuning curves but different response properties, and both receive parallel input from OSNs. Mitral cell output (Mi_{out}) is additionally shaped by PG-mediated dendrodendritic inhibition, such that only the most strongly excited mitral cells are activated, while more weakly excited mitral cells exhibit net inhibitory responses (Cleland and Sethupathy, 2006). The shape of the Mi_{out} curve generates the familiar on-center/inhibitory-surround function of contrast enhancement (*inset*).

as well as themselves (Isaacson and Strowbridge, 1998), although the region receiving this inhibition is not clearly localized (Debarbieux et al., 2003; Djurisic et al., 2004; Luo and Katz, 2001). Subsequent models proposed that contrast enhancement was instead mediated by lateral inhibition mediated by the relatively superficial periglomerular (PG) cells (Linster and Gervais, 1996; Linster and Hasselmo, 1997) (**Figs. 1**A and **2**B). This hypothesis offered the substantial advantage that lateral inhibition could be delivered onto mitral cells in the glomerular region of their apical dendrites, a location better capable of preventing spike initiation in these cells. In a model based on this hypothesis, Linster and Hasselmo (1997) further showed that if the activation of PG cells is modulated by cholinergic inputs from the horizontal limb of the diagonal band, a relatively stable number of active mitral cells can be maintained independent of the intensity of olfactory input or the set of OSNs activated by the odorant. In this model, granule cells served instead to modulate the gain of mitral cell activity, and were necessary in order to obtain stable average firing rates. Indeed, subsequent studies have shown that PG cells are appropriately modulated by acetylcholine (Castillo et al., 1999), and some of the behavioral predictions from these models have been tested in rats (Linster and Cleland, 2002; Linster et al., 2003).

However, these models still suffer from the limitation that nearest-neighbor inhibitory interactions do not appropriately map onto similarities in the molecular receptive ranges of glomeruli or their constituent OSNs (Cleland, 2010; Cleland and Sethupathy, 2006; Soucy et al., 2009). Contrast enhancement, the effects of which have been observed in the olfactory bulb (Yokoi et al., 1995), can be functionally defined as a process of competition between neurons proportional to the similarity of the information that they mediate. Simplified models of the olfactory system, based on one-dimensional odor subspaces, have been able to implement contrast enhancement using lateral inhibition (Cleland and Linster, 2002; Linster and Cleland, 2001; Linster and Gervais, 1996; Linster and Hasselmo, 1997, 1999; Linster and Smith, 1997), and have been effective at interpreting behavioral and physiological data derived from single monotonically varying odorant series (Cleland et al., 2002, 2009; Cleland and Narla, 2003; Linster and Hasselmo, 1999; Yokoi et al., 1995). However, to escape this limitation and model more realistic, high-dimensional odor spaces (Alkasab et al., 2002; Cleland, 2014; Hudson, 1999; Korsching, 2001), subsequent models have relied upon networks constructed so that the strength of PG-mediated inhibition is effectively proportional to receptive field similarity rather than the physical proximity of glomeruli. Networks based on this assumption have been shown to best reproduce calcium imaging data obtained from honeybee OSNs and projection neurons (analogous to mitral cells), while networks based on decremental lateral inhibition performed comparably to networks based on random inhibitory projections (Linster et al., 2005). Another such model has successfully reproduced mixture processing properties measured in rats (Linster and Cleland, 2004; Wiltrout et al., 2003). Finally, non-topographical models take an entirely different approach to olfactory contrast enhancement, relying solely on intraglomerular computations and broad feedback inhibition to effect contrast enhancement via a "winner-take-most" algorithm (Fig. 2C) (Cleland, 2014; Cleland et al., 2007; Cleland and Linster, 2012; Cleland and Sethupathy, 2006). This approach does not rely on odorant feature similarities being embedded into bulbar odor maps a priori, as it is independent of the physical location of glomeruli and of specific lateral inhibitory projections. Rather, the maps of stimulus feature similarity that underlie contrast enhancement are naturally inherited from the cross-activation patterns of OSNs by odorants. This property renders this contrast enhancement algorithm uniquely robust to changing or unpredictable chemosensory environments (Cleland, 2014; Linster and Cleland, 2010).

Recent experiments analyzing the role of adult-born granule cells in olfactory learning suggest a role for these deeper interneurons for odor discrimination and contrast as well. Specifically, the rewiring of granule cell networks in response to olfactory inputs underlies changes in odor perception following perceptual leaning via passive exposure to odorants (Mandairon et al., 2018; Moreno et al., 2009). These changes in perception can arise due to increased inhibitory efficacy in the circuit (Mandairon et al., 2006) as well as through the specific rewiring of adult-born granule cells in an activity-dependent manner (Chow et al., 2012; Sailor et al., 2016). Recent modeling work suggests that the convergence of afferent and top-down information converging on these interneurons is an important determinant of the integration of adult-born neurons into olfactory bulb circuitry (Adams et al., 2019).

3.33.4   Mechanisms Underlying Oscillations and Spike Synchronization

While recent models favor glomerular-layer mechanisms for contrast enhancement, granule cell activity also clearly shapes mitral cell response patterns, and hence the presumptive odor representations that emerge from the olfactory bulb. Specifically, several computational models of the olfactory bulb have suggested that the temporal pattern of spiking among mitral cells may play a role in odor representation (Meredith, 1992; Schild, 1988; White et al., 1998; White et al., 1992; White and Kauer, 2001). While it is clear that temporal response patterns in mitral cells do change as a function of odor identity (Fig. 3A), there is as yet no broadly accepted theory of how these response patterns may contribute to the representation of odorant stimuli.

One of the most widely studied features of olfactory bulb processing has been the dynamic oscillatory activity patterns observed in the bulb in response to odor stimulation. Models of these phenomena have traditionally studied these responses as coupled oscillators, attributing the dynamics in whole or in part to reciprocal feedback interactions between mitral cell secondary dendrites and granule cells (Fig. 3B) (de Almeida et al., 2013; Erdi et al., 1993; Ermentrout and Kleinfeld, 2001; Freeman, 1979; Freeman, 1987; Freeman, 1994; Grobler and Erdi, 1991; Li and Cleland, 2013; Li and Cleland, 2017; Li and Hopfield, 1989; Linster et al., 2011). Some researchers have proposed that odor quality may be represented in dynamic attractors formed in the olfactory bulb (Breakspear, 2001; Erdi et al., 1993; Freeman, 1979, 1987, 1994; Fukai, 1996; Hoshino et al., 1998; Li and Hopfield, 1989). Modulation of oscillatory dynamics may underlie changes in odor perception as observed in behavioral experiments manipulating noradrenergic and cholinergic activity in the olfactory bulb by changing synchronization patterns (de Almeida et al., 2013; de Almeida et al., 2015; Devore et al., 2014; Escanilla et al., 2010; Li and Cleland, 2013). However, it is increasingly clear that the dynamics of the olfactory bulb are tightly coupled with those of the piriform cortex, and that both depend on mutual feedback between the two structures (Gray and Skinner, 1988; Kay, 2014; Kay and Lazzara, 2010; Martin et al., 2004; Neville and Haberly, 2003; Osinski and Kay, 2016); combined bulb-cortex models have suggested possible roles for these interactions (Barreiro et al., 2017; de Almeida et al., 2013, 2015; Fukai, 1996; Grabska-Barwinska et al., 2017; Li and Hertz, 2000). Other aspects of piriform cortical dynamics have also been modeled (Claverol et al., 2002; Liljenstrom and Hasselmo, 1995; Wilson and Bower, 1992; Xu and Principe, 2004), albeit with less focus on their functional role (but see (Granger and Lynch, 1991).

Recently, models of these field oscillatory properties have begun to emphasize their relationship to the regulation of spike timing in mitral cells (Davison et al., 2003; Margrie and Schaefer, 2003), suggesting that patterns of spike synchronization among mitral cells responding to the same sensory input are important contributors to the odorant representation at this level (Fig. 3C). This phenomenon has been extensively modeled in the insect antennal lobe, a functionally comparable analog of the olfactory bulb
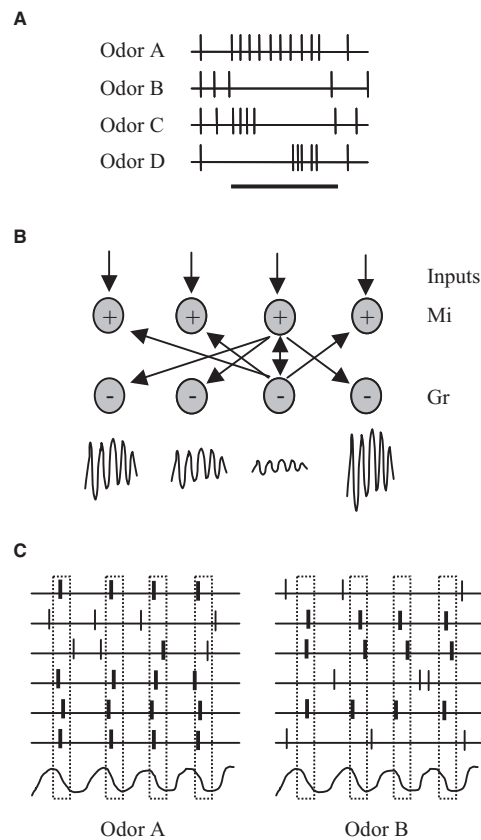
Figure 3   Oscillations and synchrony. (A) Any given mitral cell in the olfactory bulb may respond to different odorant stimuli (A–D) with a variety of temporally complex spike patterns including interwoven excitatory and inhibitory phases. It has been proposed that these temporal patterns may contribute to odor representations in the vertebrate olfactory bulb and the analogous insect antennal lobe (Laurent, 1999; Laurent et al., 2001). Horizontal bar depicts the time of odorant presentation. (B) The reciprocal synaptic interactions between mitral (Mi) and granule (Gr) cells have often been simulated as a system of coupled oscillators driven by external inputs. In such models, variance of stimulus amplitudes across these inputs generates a map of field oscillations with variable amplitudes and fixed phase lags across the olfactory bulb. For clarity, the output from only a single column is depicted. (C) Field oscillatory dynamics are believed to reflect and/or influence spike timing in mitral cells, potentially resulting in odor-specific populations of mitral cells based on spike synchrony rather than overall activity. While the overall activity patterns evoked by odors A and B are very similar, selection for spikes relatively synchronized with one another and with the oscillatory field potential reveals two clearly odor-specific subpopulations (bold spikes within dotted boxes).

(Bazhenov et al., 2001a,b; Laurent et al., 2001; Stopfer et al., 1997). In these models, the regulation of spike synchronization among secondary neurons can mediate stimulus salience and contrast enhancement between similar odorants (Cleland and Linster, 2002; Linster and Cleland, 2001), and can dramatically influence the readout of information at the next level of processing (Sivan and Kopell, 2004). Olfactory bulb temporal codes, reflecting specific sequences of principal neurons activated by an odor, can represent odor quality and be read by specific models of piriform cortex (Stern et al., 2018; Wilson et al., 2017).

3.33.5   Odor Segmentation and Associative Memory Function

Odor segmentation is the general term for the problem of how the olfactory system is able to segregate and identify different odorants that are encountered simultaneously. As most odors comprise multiple separate odorant molecules, it is far from clear how the olfactory system can parse the multitude of odorant stimuli present at any given time and attribute each to appropriately separate sources. One approach has been to hypothesize that odors emitted from different sources can be segregated by OB circuitry based upon their differential fluctuations in time (Fort and Rospars, 1992; Hendin et al., 1998; Hopfield, 1999). Odor segmentation could thereafter be performed in the OB using source-separation algorithms dependent upon associative memory function. Generally, such models hypothesize that associative memories for patterns of olfactory bulb activity evoked by known odorants become embedded in bulbar circuitry, and can then be used to recognize these patterns when they recur, even in degraded form. Specifically, a model by Hendin et al. (1998) illustrates how, if the glomerular layer feeds into a mitral-granule cell layer for which appropriate dynamics for an associative memory function have been implemented, each odor can be separately represented in successive inhalation cycles when multiple (known) odors are presented at the same time.
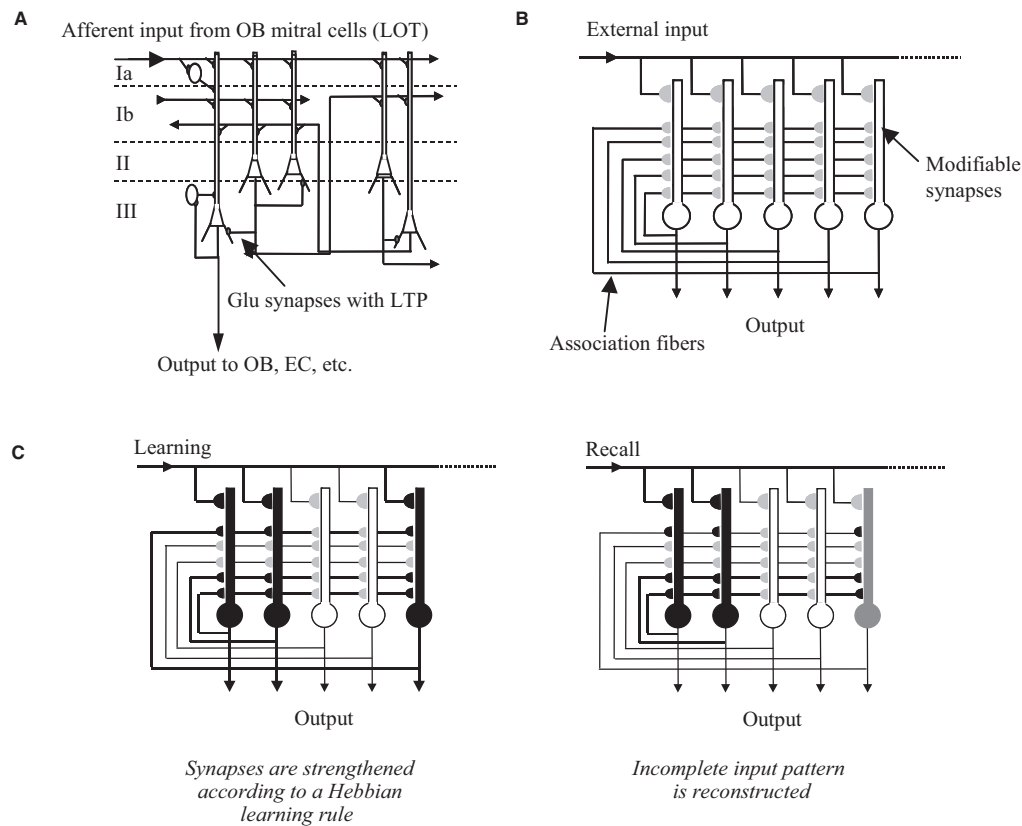
Figure 4   Associative memory function in olfactory cortex. (A) Piriform cortex (PC) exhibits the fundamental anatomical features necessary for the implementation of associative memory: extrinsic input from the olfactory bulb (OB) to each pyramidal cell via the lateral olfactory tract (LOT) and extensive intrinsic excitatory connections among pyramidal cells. These intrinsic associative connections are subject to synaptic plasticity, also crucial for associative memory function, and exhibit long-term potentiation (LTP). Additionally, several classes of local inhibitory interneurons have been described in the piriform cortex. Piriform pyramidal neurons project back to the OB, as well as to other structures such as the entorhinal cortex (EC). (B) Schematic representation of an associative memory network. The critical features are (1) external inputs to associative neurons, (2) all-to-all excitatory connections among these neurons, and (3) a learning rule that modifies the strengths of these connections when external inputs are being learned by the network. (C) Learning and recall in an associative memory network. *Learning* (left panel). An olfactory stimulus activates a subset of pyramidal cells (three dark cells) via distributed afferent projections from the OB to the PC. During learning, excitatory synaptic connections between pyramidal cells activated by that odorant are strengthened via a hebbian plasticity rule (dark semicircles denote strengthened synapses). *Recall* (right panel). After learning of a pattern, if a noisy or degraded example of that pattern is presented to the system, the stored odorant pattern can be reconstructed due to the previously strengthened connections. Dark semicircles denote strengthened synapses. Owing to the previously strengthened synapses, activation of the two dark cells secondarily activates a third cell (gray), reconstructing the previously learned pattern.

Olfactory associative memory functions have been more commonly attributed to the piriform cortex, one of the targets of mitral cell axons projecting from the olfactory bulb (Fig. 4). Specifically, the piriform cortex has been proposed to mediate the associative memory functions necessary for odor-context learning (Haberly, 2001; Haberly and Bower, 1989; Hasselmo et al., 1990) and hierarchical clustering (Ambros-Ingerson et al., 1990). Indeed, the extensive intrinsic feedback network in this cortex and its integration with afferent inputs closely resembles the structure of traditional theoretical associative memory networks as first described by Marr (1971). Several laboratories have constructed models of piriform cortex implementing these associative memory functions (Ambros-Ingerson et al., 1990; Barkai and Hasselmo, 1994; Haberly and Bower, 1989; Hasselmo et al., 1997; Hasselmo et al., 1990) as well as exploring the role of cholinergic modulation in their regulation (Hasselmo et al., 1990, 1997; Linster and Hasselmo, 2001; Linster et al., 2003; Patil and Hasselmo, 1999). Later work with combined olfactory bulb-cortex models has explored to what extent bulbar representations and dynamics contribute to cortical learning, and tested hypotheses from these models experimentally (de Almeida et al., 2013, 2015, 2016; Devore et al., 2014; Stern et al., 2018).

3.33.6   Detailed Biophysical Models of OB Neurons

Most models of the olfactory system to date have emphasized network-level interactions and the properties of olfactory bulb and piriform cortical circuitry, using simplified cell models conducive to these larger-scale simulations. However, several relatively

detailed biophysical models of olfactory neurons – particularly OSNs and mitral cells –also have been constructed. Several detailed OSN models have illustrated how ligand-receptor binding and nonlinear transduction processes can underlie several experimentally observed response properties of these cells (Cleland and Linster, 1999; Kaissling, 1998, 2001; Kaissling and Rospars, 2004; Lansky and Rospars, 1998; Malaka et al., 1995; Rospars et al., 2000; Rospars et al., 1996; Vermeulen et al., 1997; Vermeulen and Rospars, 1998; Vermeulen et al., 1996). Compartmental models of mitral cells have been used to elucidate intrinsic cellular phenomena, such as the localization of spike initiation in mitral cells (Chen et al., 2002; Shen et al., 1999), long-term potentiation at the OSN-mitral synapse (Ennis et al., 1998), or their intrinsic dynamics (Li and Cleland, 2017; Rubin and Cleland, 2006; Viertel and Borisyuk, 2019). Other compartmental models have focused on bridging the gap between cellular and systems properties in both vertebrate and insect systems (Bazhenov et al., 2001a; Bhalla and Bower, 1993; Cleland and Sethupathy, 2006; Davison et al., 2000; Davison et al., 2003; Li and Cleland, 2013, 2017, 2018; Li et al., 2015).

3.33.7   Summary and Conclusions

Computational models have an established and growing role within systems neuroscience. As our understanding of neural processing and interactions becomes more sophisticated, computer models of these systems are increasingly necessary in order to understand and interpret experimental results. Models serve as proofs of concept, tests of sufficiency, and as quantitative embodiments of working hypotheses. In the olfactory system in particular, computational modeling will no doubt be essential to understanding the integration of the many factors influencing the construction and transformation of odor representations. Many of the functions ascribed to olfactory networks have been proposed and analyzed using computational modeling; these guide and interpret experimental work. Specifically, the neural networks and mechanisms underlying specific functions are particularly well described using models of known networks. Biophysical models specifically have contributed to the fields thinking about mechanisms underlying oscillations in the olfactory bulb. Future directions should include coordinated computational and experimental approaches to study feedback interactions between olfactory brain areas.

References

Adams, W., Graham, J.N., Han, X., Riecke, H., 2019. Top-down inputs drive neuronal network rewiring and context-enhanced sensory processing in olfaction. PLoS Comput. Biol. 15 (1), e1006611.

Adrian, E.D., 1953. Sensory messages and sensation; the response of the olfactory organ to different smells. Acta Physiol. Scand. 29 (1), 5–14.

Alkasab, T.K., White, J., Kauer, J.S., 2002. A computational system for simulating and analyzing arrays of biological and artificial chemical sensors. Chem. Senses 27 (3), 261–275.

Ambros-Ingerson, J., Granger, R., Lynch, G., 1990. Simulation of paleocortex performs hierarchical clustering. Science 247 (4948), 1344–1348.

Anton, P.S., Lynch, G., Granger, R., 1991. Computation of frequency-to-spatial transform by olfactory bulb glomeruli. Biol. Cybern. 65 (5), 407–414.

Barkai, E., Hasselmo, M.E., 1994. Modulation of the input/output function of rat piriform cortex pyramidal cells. J. Neurophysiol. 72 (2), 644–658.

Barreiro, A.K., Gautam, S.H., Shew, W.L., Ly, C., 2017. A theoretical framework for analyzing coupled neuronal networks: application to the olfactory system. PLoS Comput. Biol. 13 (10), e1005780.

Bazhenov, M., Stopfer, M., Rabinovich, M., Abarbanel, H.D., Sejnowski, T.J., Laurent, G., 2001a. Model of cellular and network mechanisms for odor-evoked temporal patterning in the locust antennal lobe. Neuron 30 (2), 569–581.

Bazhenov, M., Stopfer, M., Rabinovich, M., Huerta, R., Abarbanel, H.D., Sejnowski, T.J., Laurent, G., 2001b. Model of transient oscillatory synchronization in the locust antennal lobe. Neuron 30 (2), 553–567.

Bhalla, U.S., Bower, J.M., 1993. Exploring parameter space in detailed single neuron models: simulations of the mitral and granule cells of the olfactory bulb. J. Neurophysiol. 69 (6), 1948–1965.

Bozza, T., Feinstein, P., Zheng, C., Mombaerts, P., 2002. Odorant receptor expression defines functional units in the mouse olfactory system. J. Neurosci. 22 (8), 3033–3043.

Breakspear, M., 2001. Perception of odors by a nonlinear model of the olfactory bulb. Int. J. Neural Syst. 11 (2), 101–124.

Castillo, P.E., Carleton, A., Vincent, J.D., Lledo, P.M., 1999. Multiple and opposing roles of cholinergic transmission in the main olfactory bulb. J. Neurosci. 19 (21), 9180–9191.

Chen, W.R., Shen, G.Y., Shepherd, G.M., Hines, M.L., Midtgaard, J., 2002. Multiple modes of action potential initiation and propagation in mitral cell primary dendrite. J. Neurophysiol. 88 (5), 2755–2764.

Chow, S.F., Wick, S.D., Riecke, H., 2012. Neurogenesis drives stimulus decorrelation in a model of the olfactory bulb. PLoS Comput. Biol. 8 (3), e1002398.

Claverol, E.T., Brown, A.D., Chad, J.E., 2002. A large-scale simulation of the piriform cortex by a cell automaton-based network model. IEEE Trans. Biomed. Eng. 49 (9), 921–935.

Cleland, T.A., 2010. Early transformations in odor representation. Trends Neurosci. 33 (3), 130–139.

Cleland, T.A., 2014. Construction of odor representations by olfactory bulb microcircuits. Prog. Brain Res. 208, 177–203.

Cleland, T.A., Chen, S.Y., Hozer, K.W., Ukatu, H.N., Wong, K.J., Zheng, F., 2011. Sequential mechanisms underlying concentration invariance in biological olfaction. Front. Neuroeng. 4, 21.

Cleland, T.A., Johnson, B.A., Leon, M., Linster, C., 2007. Relational representation in the olfactory system. Proc. Natl. Acad. Sci. U. S. A. 104 (6), 1953–1958.

Cleland, T.A., Linster, C., 1999. Concentration tuning mediated by spare receptor capacity in olfactory sensory neurons: a theoretical study. Neural Comput. 11 (7), 1673–1690.

Cleland, T.A., Linster, C., 2002. How synchronization properties among second-order sensory neurons can mediate stimulus salience. Behav. Neurosci. 116 (2), 212–221.

Cleland, T.A., Linster, C., 2003. Central olfactory processing. In: Doty, R.L. (Ed.), Handbook of Olfaction and Gustation, second ed. Marcel Dekker, New York, pp. 165–180.

Cleland, T.A., Linster, C., 2012. On-center/inhibitory-surround decorrelation via intraglomerular inhibition in the olfactory bulb glomerular layer. Front. Integr. Neurosci. 6, 5.

Cleland, T.A., Morse, A., Yue, E.L., Linster, C., 2002. Behavioral models of odor similarity. Behav. Neurosci. 116 (2), 222–231.

Cleland, T.A., Narla, V.A., 2003. Intensity modulation of olfactory acuity. Behav. Neurosci. 117 (6), 1434–1440.

Cleland, T.A., Narla, V.A., Boudadi, K., 2009. Multiple learning parameters differentially regulate olfactory generalization. Behav. Neurosci. 123 (1), 26–35.

Cleland, T.A., Sethupathy, P., 2006. Non-topographical contrast enhancement in the olfactory bulb. BMC Neurosci. 7, 7.

Davison, A.P., Feng, J., Brown, D., 2000. A reduced compartmental model of the mitral cell for use in network models of the olfactory bulb. Brain Res. Bull. 51 (5), 393–399.

Davison, A.P., Feng, J., Brown, D., 2003. Dendrodendritic inhibition and simulated odor responses in a detailed olfactory bulb network model. J. Neurophysiol. 90 (3), 1921–1935.

de Almeida, L., Idiart, M., Dean, O., Devore, S., Smith, D.M., Linster, C., 2016. Internal cholinergic regulation of learning and recall in a model of olfactory processing. Front. Cell. Neurosci. 10, 256.

de Almeida, L., Idiart, M., Linster, C., 2013. A model of cholinergic modulation in olfactory bulb and piriform cortex. J. Neurophysiol. 109 (5), 1360–1377.

de Almeida, L., Reiner, S.J., Ennis, M., Linster, C., 2015. Computational modeling suggests distinct, location-specific function of norepinephrine in olfactory bulb and piriform cortex. Front. Comput. Neurosci. 9, 73.

Debarbieux, F., Audinat, E., Charpak, S., 2003. Action potential propagation in dendrites of rat mitral cells in vivo. J. Neurosci. 23 (13), 5553–5560.

Devore, S., de Almeida, L., Linster, C., 2014. Distinct roles of bulbar muscarinic and nicotinic receptors in olfactory discrimination learning. J. Neurosci. 34 (34), 11244–11260.

Djurisic, M., Antic, S., Chen, W.R., Zecevic, D., 2004. Voltage imaging from dendrites of mitral cells: EPSP attenuation and spike trigger zones. J. Neurosci. 24 (30), 6703–6714.

Duchamp-Viret, P., Duchamp, A., Vigouroux, M., 1989. Amplifying role of convergence in olfactory system a comparative study of receptor cell and second-order neuron sensitivities. J. Neurophysiol. 61 (5), 1085–1094.

Ennis, M., Linster, C., Aroniadou-Anderjaska, V., Ciombor, K., Shipley, M.T., 1998. Glutamate and synaptic plasticity at mammalian primary olfactory synapses. Ann. N. Y. Acad. Sci. 855, 457–466.

Erdi, P., Grobler, T., Barna, G., Kaski, K., 1993. Dynamics of the olfactory bulb: bifurcations, learning, and memory. Biol. Cybern. 69 (1), 57–66.

Ermentrout, G.B., Kleinfeld, D., 2001. Traveling electrical waves in cortex: insights from phase dynamics and speculation on a computational role. Neuron 29 (1), 33–44.

Escanilla, O., Arrellanos, A., Karnow, A., Ennis, M., Linster, C., 2010. Noradrenergic modulation of behavioral odor detection and discrimination thresholds in the olfactory bulb. Eur. J. Neurosci. 32 (3), 458–468.

Fletcher, M.L., Bendahmane, M., 2014. Visualizing olfactory learning functional imaging of experience-induced olfactory bulb changes. Prog. Brain Res. 208, 89–113.

Fort, J.C., Rospars, J.P., 1992. Modelling of the qualitative discrimination of odours in the first two layers of olfactory system by Jutten and Herault algorithm. C R Acad. Sci. III 315 (9), 331–336.

Freeman, W.J., 1979. Nonlinear dynamics of paleocortex manifested in the olfactory EEG. Biol. Cybern. 35 (1), 21–37.

Freeman, W.J., 1987. Simulation of chaotic EEG patterns with a dynamic model of the olfactory system. Biol. Cybern. 56 (2–3), 139–150.

Freeman, W.J., 1994. Characterization of state transitions in spatially distributed, chaotic, nonlinear, dynamical systems in cerebral cortex. Integr. Physiol. Behav. Sci. 29 (3), 294–306.

Friedrich, R.W., Korsching, S.I., 1997. Combinatorial and chemotopic odorant coding in the zebrafish olfactory bulb visualized by optical imaging. Neuron 18 (5), 737–752.

Fukai, T., 1996. Bulbo cortical interplay in olfactory information processing via synchronous oscillations. Biol. Cybern. 74 (4), 309–317.

Grabska-Barwinska, A., Barthelme, S., Beck, J., Mainen, Z.F., Pouget, A., Latham, P.E., 2017. A probabilistic approach to demixing odors. Nat. Neurosci. 20 (1), 98–106.

Granger, R., Lynch, G., 1991. Higher olfactory processes: perceptual learning and memory. Curr. Opin. Neurobiol. 1 (2), 209–214.

Gray, C.M., Skinner, J.E., 1988. Centrifugal regulation of neuronal activity in the olfactory bulb of the waking rabbit as revealed by reversible cryogenic blockade. Exp. Brain Res. 69 (2), 378–386.

Grobler, T., Erdi, P., 1991. Dynamic phenomena in the olfactory bulb. Acta Biochim. Biophys. Hung. 26 (1–4), 61–65.

Haberly, L.B., 2001. Parallel-distributed processing in olfactory cortex: new insights from morphological and physiological analysis of neuronal circuitry. Chem. Senses 26 (5), 551–576.

Haberly, L.B., Bower, J.M., 1989. Olfactory cortex: model circuit for study of associative memory? Trends Neurosci. 12 (7), 258–264.

Hasselmo, M.E., Linster, C., Patil, M., Ma, D., Cekic, M., 1997. Noradrenergic suppression of synaptic transmission may influence cortical signal-to-noise ratio. J. Neurophysiol. 77 (6), 3326–3339.

Hasselmo, M.E., Wilson, M.A., Anderson, B.P., Bower, J.M., 1990. Associative memory function in piriform (olfactory) cortex: computational modeling and neuropharmacology. Cold Spring Harb. Symp. Quant. Biol. 55, 599–610.

Hendin, O., Horn, D., Tsodyks, M.V., 1998. Associative memory and segmentation in an oscillatory neural model of the olfactory bulb. J. Comput. Neurosci. 5 (2), 157–169.

Hopfield, J.J., 1999. Odor space and olfactory processing: collective algorithms and neural implementation. Proc. Natl. Acad. Sci. U. S. A. 96 (22), 12506–12511.

Hoshino, O., Kashimori, Y., Kambara, T., 1998. An olfactory recognition model based on spatio-temporal encoding of odor quality in the olfactory bulb. Biol. Cybern. 79 (2), 109–120.

Hudson, R., 1999. From molecule to mind: the role of experience in shaping olfactory function. J Comp. Physiol. A 185 (4), 297–304.

Isaacson, J.S., Strowbridge, B.W., 1998. Olfactory reciprocal synapses: dendritic signaling in the CNS. Neuron 20 (4), 749–761.

Kaissling, K.E., 1998. A quantitative model of odor deactivation based on the redox shift of the pheromone-binding protein im moth antennae. Ann. N. Y. Acad. Sci. 855, 320–322.

Kaissling, K.E., 2001. Olfactory perireceptor and receptor events in moths: a kinetic model. Chem. Senses 26 (2), 125–150.

Kaissling, K.E., Rospars, J.P., 2004. Dose-response relationships in an olfactory flux detector model revisited. Chem. Senses 29 (6), 529–531.

Kauer, J.S., 1991. Contributions of topography and parallel processing to odor coding in the vertebrate olfactory pathway. Trends Neurosci. 14 (2), 79–85.

Kay, L.M., 2014. Circuit oscillations in odor perception and memory. Prog. Brain Res. 208, 223–251.

Kay, L.M., Lazzara, P., 2010. How global are olfactory bulb oscillations? J. Neurophysiol. 104 (3), 1768–1773.

Korsching, S.I., 2001. Odor maps in the brain: spatial aspects of odor representation in sensory surface and olfactory bulb. Cell. Mol. Life Sci. 58 (4), 520–530.

Lansky, P., Rospars, J.P., 1998. Odorant concentration and receptor potential in olfactory sensory neurons. Biosystems 48 (1–3), 131–138.

Laurent, G., 1999. A systems perspective on early olfactory coding. Science 286 (5440), 723–728.

Laurent, G., Stopfer, M., Friedrich, R.W., Rabinovich, M.I., Volkovskii, A., Abarbanel, H.D., 2001. Odor encoding as an active, dynamical process: experiments, computation, and theory. Annu. Rev. Neurosci. 24, 263–297.

Li, G., Cleland, T.A., 2013. A two-layer biophysical model of cholinergic neuromodulation in olfactory bulb. J. Neurosci. 33 (7), 3037–3058.

Li, G., Cleland, T.A., 2017. A coupled-oscillator model of olfactory bulb gamma oscillations. PLoS Comput. Biol. 13 (11), e1005760.

Li, G., Cleland, T.A., 2018. Generative biophysical modeling of dynamical networks in the olfactory system. Methods Mol. Biol. 1820, 265–288.

Li, G., Linster, C., Cleland, T.A., 2015. Functional differentiation of cholinergic and noradrenergic modulation in a biophysical model of olfactory bulb granule cells. J. Neurophysiol. 114 (6), 3177–3200.

Li, Z., Hertz, J., 2000. Odour recognition and segmentation by a model olfactory bulb and cortex. Network 11 (1), 83–102.

Li, Z., Hopfield, J.J., 1989. Modeling the olfactory bulb and its neural oscillatory processings. Biol. Cybern. 61 (5), 379–392.

Liljenstrom, H., Hasselmo, M.E., 1995. Cholinergic modulation of cortical oscillatory dynamics. J. Neurophysiol. 74 (1), 288–297.

Linster, C., Cleland, T.A., 2001. How spike synchronization among olfactory neurons can contribute to sensory discrimination. J. Comput. Neurosci. 10 (2), 187–193.

Linster, C., Cleland, T.A., 2002. Cholinergic modulation of sensory representations in the olfactory bulb. Neural Network. 15 (4–6), 709–717.

Linster, C., Cleland, T.A., 2004. Configurational and elemental odor mixture perception can arise from local inhibition. J. Comput. Neurosci. 16 (1), 39–47.

Linster, C., Cleland, T.A., 2010. Decorrelation of odor representations via spike timing-dependent plasticity. Front. Comput. Neurosci. 4, 157.

Linster, C., Gervais, R., 1996. Investigation of the role of interneurons and their modulation by centrifugal fibers in a neural model of the olfactory bulb. J. Comput. Neurosci. 3 (3), 225–246.

Linster, C., Hasselmo, M., 1997. Modulation of inhibition in a model of olfactory bulb reduces overlap in the neural representation of olfactory stimuli. Behav. Brain Res. 84 (1–2), 117–127.

Linster, C., Hasselmo, M.E., 1999. Behavioral responses to aliphatic aldehydes can be predicted from known electrophysiological responses of mitral cells in the olfactory bulb. Physiol. Behav. 66 (3), 497–502.

Linster, C., Hasselmo, M.E., 2001. Neuromodulation and the functional dynamics of piriform cortex. Chem. Senses 26 (5), 585–594.

Linster, C., Johnson, B.A., Morse, A., Yue, E., Leon, M., 2002. Spontaneous versus reinforced olfactory discriminations. J. Neurosci. 22 (16), 6842–6845.

Linster, C., Johnson, B.A., Yue, E., Morse, A., Xu, Z., Hingco, E.E., Choi, Y., Choi, M., Messiha, A., Leon, M., 2001. Perceptual correlates of neural representations evoked by odorant enantiomers. J. Neurosci. 21 (24), 9837–9843.

Linster, C., Maloney, M., Patil, M., Hasselmo, M.E., 2003. Enhanced cholinergic suppression of previously strengthened synapses enables the formation of self-organized representations in olfactory cortex. Neurobiol. Learn. Mem. 80 (3), 302–314.

Linster, C., Nai, Q., Ennis, M., 2011. Nonlinear effects of noradrenergic modulation of olfactory bulb function in adult rodents. J. Neurophysiol. 105 (4), 1432–1443.

Linster, C., Sachse, S., Galizia, G., 2005. Computational modeling suggests that response properties rather than spatial position determine connectivity between olfactory glomeruli. J. Neurophysiol. 93 (6), 3410–3417.

Linster, C., Smith, B.H., 1997. A computational model of the response of honey bee antennal lobe circuitry to odor mixtures: overshadowing, blocking and unblocking can arise from lateral inhibition. Behav. Brain Res. 87 (1), 1–14.

Lowe, G., Gold, G.H., 1995. Olfactory transduction is intrinsically noisy. Proc. Natl. Acad. Sci. U. S. A. 92 (17), 7864–7868.

Luo, M., Katz, L.C., 2001. Response correlation maps of neurons in the mammalian olfactory bulb. Neuron 32 (6), 1165–1179.

Malaka, R., Ragg, T., Hammer, M., 1995. Kinetic models of odor transduction implemented as artificial neural networks. Simulations of complex response properties of honeybee olfactory neurons. Biol. Cybern. 73 (3), 195–207.

Mandairon, N., Kuczewski, N., Kermen, F., Forest, J., Midroit, M., Richard, M., Thevenet, M., Sacquet, J., Linster, C., Didier, A., 2018. Opposite regulation of inhibition by adult-born granule cells during implicit versus explicit olfactory learning. ELife 7, e34976.

Mandairon, N., Stack, C., Kiselycznyk, C., Linster, C., 2006. Broad activation of the olfactory bulb produces long-lasting changes in odor perception. Proc. Natl. Acad. Sci. U. S. A. 103 (36), 13543–13548.

Margrie, T.W., Schaefer, A.T., 2003. Theta oscillation coupled spike latencies yield computational vigour in a mammalian sensory system. J. Physiol. 546 (Pt 2), 363–374.

Marr, D., 1971. Simple memory: a theory for archicortex. Philos. Trans. R. Soc. Lond. B Biol. Sci. 262 (841), 23–81.

Martin, C., Gervais, R., Hugues, E., Messaoudi, B., Ravel, N., 2004. Learning modulation of odor-induced oscillatory responses in the rat olfactory bulb: a correlate of odor recognition? J. Neurosci. 24 (2), 389–397.

Meisami, E., 1989. A proposed relationship between increases in the number of olfactory receptor neurons, convergence ratio and sensitivity in the developing rat. Brain Res. Dev. Brain Res. 46 (1), 9–19.

Meister, M., Bonhoeffer, T., 2001. Tuning and topography in an odor map on the rat olfactory bulb. J. Neurosci. 21 (4), 1351–1360.

Meredith, M., 1992. Neural circuit computation: complex patterns in the olfactory bulb. Brain Res. Bull. 29 (1), 111–117.

Mombaerts, P., 1996. Targeting olfaction. Curr. Opin. Neurobiol. 6 (4), 481–486.

Moreno, M.M., Linster, C., Escanilla, O., Sacquet, J., Didier, A., Mandairon, N., 2009. Olfactory perceptual learning requires adult neurogenesis. Proc. Natl. Acad. Sci. U. S. A. 106 (42), 17980–17985.

Moulton, D.G., 1967. Spatio-temporal patterning of response in the olfactory system. In: Hayashi, T. (Ed.), Olfaction and Taste II. Pergamon Press, New York, pp. 109–116.

Nagayama, S., Homma, R., Imamura, F., 2014. Neuronal organization of olfactory bulb circuits. Front. Neural Circ. 8, 98.

Neville, K.R., Haberly, L.B., 2003. Beta and gamma oscillations in the olfactory system of the urethane-anesthetized rat. J. Neurophysiol. 90 (6), 3921–3930.

Osinski, B.L., Kay, L.M., 2016. Granule cell excitability regulates gamma and beta oscillations in a model of the olfactory bulb dendrodendritic microcircuit. J. Neurophysiol. 116 (2), 522–539.

Patil, M.M., Hasselmo, M.E., 1999. Modulation of inhibitory synaptic potentials in the piriform cortex. J. Neurophysiol. 81 (5), 2103–2118.

Rall, W., Shepherd, G.M., 1968. Theoretical reconstruction of field potentials and dendrodendritic synaptic interactions in olfactory bulb. J. Neurophysiol. 31 (6), 884–915.

Rospars, J.P., Lansky, P., Duchamp-Viret, P., Duchamp, A., 2000. Spiking frequency versus odorant concentration in olfactory receptor neurons. Biosystems 58 (1–3), 133–141.

Rospars, J.P., Lansky, P., Tuckwell, H.C., Vermeulen, A., 1996. Coding of odor intensity in a steady-state deterministic model of an olfactory receptor neuron. J. Comput. Neurosci. 3 (1), 51–72.

Rubin, B.D., Katz, L.C., 1999. Optical imaging of odorant representations in the mammalian olfactory bulb. Neuron 23 (3), 499–511.

Rubin, D.B., Cleland, T.A., 2006. Dynamical mechanisms of odor processing in olfactory bulb mitral cells. J. Neurophysiol. 96 (2), 555–568.

Sailor, K.A., Valley, M.T., Wiechert, M.T., Riecke, H., Sun, G.J., Adams, W., Dennis, J.C., Sharafi, S., Ming, G.L., Song, H., Lledo, P.M., 2016. Persistent structural plasticity optimizes sensory information processing in the olfactory bulb. Neuron 91 (2), 384–396.

Schild, D., 1988. Principles of odor coding and a neural network for odor discrimination. Biophys. J. 54 (6), 1001–1011.

Schoenfeld, T.A., Knott, T.K., 2004. Evidence for the disproportionate mapping of olfactory airspace onto the main olfactory bulb of the hamster. J. Comp. Neurol. 476 (2), 186–201.

Shen, G.Y., Chen, W.R., Midtgaard, J., Shepherd, G.M., Hines, M.L., 1999. Computational analysis of action potential initiation in mitral cell soma and dendrites based on dual patch recordings. J. Neurophysiol. 82 (6), 3006–3020.

Shepard, R.N., 1987. Toward a universal law of generalization for psychological science. Science 237 (4820), 1317–1323.

Shepard, R.N., Chang, J.J., 1963. Stimulus generalization in the learning of classifications. J. Exp. Psychol. 65, 94–102.

Shepherd, G.M., Brayton, R.K., 1979. Computer simulation of a dendrodendritic synaptic circuit for self- and lateral-inhibition in the olfactory bulb. Brain Res. 175 (2), 377–382.

Sivan, E., Kopell, N., 2004. Mechanism and circuitry for clustering and fine discrimination of odors in insects. Proc. Natl. Acad. Sci. U. S. A. 101 (51), 17861–17866.

Soucy, E.R., Albeanu, D.F., Fantana, A.L., Murthy, V.N., Meister, M., 2009. Precision and diversity in an odor map on the olfactory bulb. Nat. Neurosci. 12 (2), 210–220.

Stern, M., Bolding, K.A., Abbott, L.F., Franks, K.M., 2018. A transformation from temporal to ensemble coding in a model of piriform cortex. ELife 7.

Stewart, W.B., Kauer, J.S., Shepherd, G.M., 1979. Functional organization of rat olfactory bulb analysed by the 2-deoxyglucose method. J. Comp. Neurol. 185 (4), 715–734.

Stopfer, M., Bhagavan, S., Smith, B.H., Laurent, G., 1997. Impaired odour discrimination on desynchronization of odour-encoding neural assemblies. Nature 390 (6655), 70–74.

Urban, N.N., 2002. Lateral inhibition in the olfactory bulb and in olfaction. Physiol. Behav. 77 (4–5), 607–612.

van Drongelen, W., Holley, A., Doving, K.B., 1978. Convergence in the olfactory system: quantitative aspects of odour sensitivity. J. Theor. Biol. 71 (1), 39–48.

Vermeulen, A., Lansky, P., Tuckwell, H., Rospars, J.P., 1997. Coding of odour intensity in a sensory neuron. Biosystems 40 (1–2), 203–210.

Vermeulen, A., Rospars, J.P., 1998. Dendritic integration in olfactory sensory neurons: a steady-state analysis of how the neuron structure and neuron environment influence the coding of odor intensity. J. Comput. Neurosci. 5 (3), 243–266.

Vermeulen, A., Rospars, J.P., Lansky, P., Tuckwell, H.C., 1996. Coding of stimulus intensity in an olfactory receptor neuron: role of neuron spatial extent and passive dendritic backpropagation of action potentials. Bull. Math. Biol. 58 (3), 493–512.

Viertel, R., Borisyuk, A., 2019. A computational model of the mammalian external tufted cell. J. Theor. Biol. 462, 109–121.

Wachowiak, M., Cohen, L.B., Zochowski, M.R., 2002. Distributed and concentration-invariant spatial representations of odorants by receptor neuron input to the turtle olfactory bulb. J. Neurophysiol. 87 (2), 1035–1045.

White, J., Dickinson, T.A., Walt, D.R., Kauer, J.S., 1998. An olfactory neuronal network for vapor recognition in an artificial nose. Biol. Cybern. 78 (4), 245–251.

White, J., Hamilton, K.A., Neff, S.R., Kauer, J.S., 1992. Emergent properties of odor information coding in a representational model of the salamander olfactory bulb. J. Neurosci. 12 (5), 1772–1780.

White, J., Kauer, J.S., 2001. Exploring olfactory population coding using an artificial olfactory system. Prog. Brain Res. 130, 191–203.

Wilson, C.D., Serrano, G.O., Koulakov, A.A., Rinberg, D., 2017. A primacy code for odor identity. Nat. Commun. 8 (1), 1477.

Wilson, M., Bower, J.M., 1992. Cortical oscillations and temporal interactions in a computer simulation of piriform cortex. J. Neurophysiol. 67 (4), 981–995.

Wiltrout, C., Dogra, S., Linster, C., 2003. Configurational and nonconfigurational interactions between odorants in binary mixtures. Behav. Neurosci. 117 (2), 236–245.

Xu, D., Principe, J.C., 2004. Dynamical analysis of neural oscillators in an olfactory cortex model. IEEE Trans. Neural Network. 15 (5), 1053–1062.

Yokoi, M., Mori, K., Nakanishi, S., 1995. Refinement of odor molecule tuning by dendrodendritic synaptic inhibition in the olfactory bulb. Proc. Natl. Acad. Sci. U. S. A. 92 (8), 3371–3375.